

Online parameter and state estimation of lithium-ion batteries under temperature effects

Hicham Chaoui^{a,*}, Hamid Gualous^b

^a The Intelligent Robotic and Energy Systems (IRES) Research Group, Department of Electronics, Carleton University, Ottawa, ON, Canada

^b The LUSAC Laboratory, University of Caen-Basse Normandie, Cherbourg-Octeville, France



ARTICLE INFO

Article history:

Received 26 September 2016

Received in revised form

23 November 2016

Accepted 28 December 2016

Keywords:

Lyapunov stability

State-space observer

Parameter estimation

Temperature uncertainties

Lithium-ion batteries

ABSTRACT

In this paper, a hybrid estimation technique is proposed for lithium-ion batteries. This strategy makes use of state-space observer theory to reduce the complexity of the design and the stability analysis. However, the battery's parameters knowledge is required for the state-space model, which limits the performance as the battery's parameters vary. Therefore, an online parameter identification strategy is proposed to track the parameters deviation. The stability of the closed-loop estimation scheme is guaranteed by Lyapunov's direct method. Unlike other estimation techniques where temperature effects are ignored, this paper proposes a universal compensation strategy which can be used with many estimation algorithms available in the literature. The performance of the proposed scheme is validated through a set of experiments under different currents and temperatures along with comparison against an adaptive observer.

© 2016 Elsevier B.V. All rights reserved.

List of abbreviations

AC	alternating current
CCCV	Constant Current Constant Voltage
EKF	extended Kalman filter
EOL	end of life
HIL	hardware in the loop
LiFePO ₄	lithium-iron phosphate battery
NiCd	nickel cadmium
NiMH	nickel metal hydride
OCV	open circuit voltage
PF	particle filter
SOC	state of charge
SOH	state of health

1. Introduction

Lithium-ion batteries offer a higher power density and energy efficiency as opposed to other types of batteries such as lead acid,

NiMH, and NiCd [1,2]. They have received an increasing interest because of their other numerous advantages such as rapid charge capability, low steady-state float current, wide temperature operation range, small size, light weight, low self-discharge rate, long life cycle, and absence of hydrogen outgassing, which make them good candidates for many applications such as electric vehicles and laptops [3]. SOC and SOH are crucial aspects in these applications since they are considered as the battery's energy and lifetime gauge, respectively. Henceforth, a bad SOC and SOH estimation would ultimately result in damaging the battery and reducing its lifespan.

A straightforward way to estimate a battery's SOC is the Amp-hour (Ah) balancing technique, also called Coulomb counting method [4,5]. In this approach, SOC is determined by integrating through time the battery's entering and leaving currents. But, the accumulation of the start-up and current sensor errors results into a drift and poor accuracy [6]. Although this technique has some serious drawbacks, it remains the simplest approach for real-time industrial applications [4]. Another rational way to determine SOC is to use the OCV since the battery's voltage is directly correlated to its charge status [7,8]. But, this correlation holds only when the battery gets to an equilibrium state (i.e., no operation for several minutes or hours). A hybrid estimation technique consists of combining the aforementioned two methods. Thus, Coulomb counting technique is then used and whenever equilibrium is reached, a reset of the accumulated errors is performed by updating the SOC with the OCV technique. Yet, batteries cannot reach an equilibrium

* Corresponding author.

E-mail addresses: hicham.chaoui@carleton.ca (H. Chaoui), hamid.gualous@unicaen.fr (H. Gualous).

state in many applications where continuous operation is needed, which calls on the necessity of examining other SOC estimation alternatives.

Several advanced estimation strategies are proposed at the cost of a higher computational complexity [9,10]. A sliding mode observer is proposed in [11] to compensate for modeling uncertainties. In [12], the SOC is derived from the charge/discharge experimental data under different constant currents and temperatures for a NiMH battery. In [13], measured current/voltage profiles are used with an optimization procedure to estimate online the battery's parameters. As such, the model captures the battery's parameters variation. Another SOC estimation method is presented in [14] using a reduced-order state observer. But, the knowledge of battery's parameters are needed for the estimation, which reduces its precision with aging. To overcome this shortcoming, an adaptive SOC estimation strategy is proposed for lead-acid and lithium-ion batteries in [15,16], respectively. Then, a proportional-integral observer is proposed in [17] to estimate the SOC of lithium-ion batteries in electric drive vehicles. EKF has been used extensively to estimate SOC and SOH [9,18,19]. Recently, in an effort to overcome the shortcomings of Kalman filters, an adaptive EKF is suggested in [20] for SOC estimation. In [21], support vector regression is used for its approximation and generalization capability to determine the battery's SOH. Finally, online estimation of battery impedance is achieved in [22] using excitation current generated by a motor controller. But, many of the aforementioned techniques do not take into consideration the impact of temperature on the estimation which limits their use in industry. Moreover, the absence of stability proof is another factor limiting their abundance use in the vehicular industry.

Other state-space estimation techniques are based on particle filter which is a sequential Monte Carlo method that use weighted random samples (particles) to estimate the probability distribution function of any nonlinear system. Several PF-based battery SOC estimation methods are suggested in the literature for lithium-ion batteries [23–25]. In [23], the battery is considered as a nonlinear dynamic system with the SOC of the battery as the only state variable. Classical Kalman filtering approaches show limitations in handling nonlinear and non-Gaussian error distribution problems. In addition, uncertainties in the battery model parameters must be taken into account to describe the battery degradation. In [24], a model-based method is presented combining a sequential Monte Carlo filter with adaptive control to determine the cell SOC and its electric impedance. The applicability of this dual estimator is verified using measurement data acquired from a commercial LiFePO₄ cell. Due to a better handling of the hysteresis, results show the benefits of the proposed method against the estimation with an extended Kalman filter. In [25], another state estimation technique is presented for lithium-iron phosphate batteries where a PF overcomes the problem of the variance and the mean of a Gaussian probability density function by using Monte Carlo sampling.

On another aspect, soft-computing tools such as neural network and fuzzy logic systems have been acknowledged in numerous applications as robust tools for systems under uncertainties [26–29]. Several intelligent algorithms have been proposed for the SOC and SOH estimation, which have performed satisfactorily [30,31]. But, neural networks remain incapable of incorporating any human-like expertise already acquired about the dynamics of the system in hand, which is considered one of the main weaknesses of such methodologies. This weakness has been overcome in [32] with a fuzzy neural network. However, these tools achieve outstanding performance at the expense of a heavy computation. Furthermore, they are based on heuristic and tuning may not be trivial. Additionally, many soft-computing based observers lack stability proofs in several estimation applications.

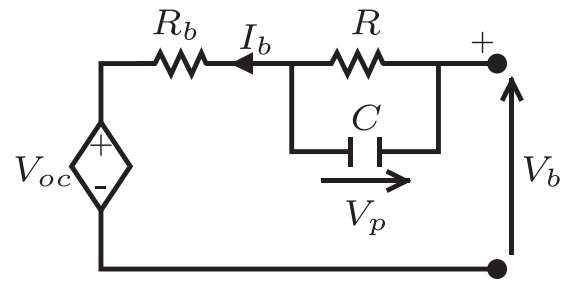


Fig. 1. Equivalent electric circuit of a lithium battery.

The battery's open circuit voltage estimation scheme is based on a state-space observer, which reduces design complexity. However, it requires the battery's parameters, which are known to be time-varying. Therefore, an adaptive parameters identification strategy is proposed using a Lyapunov-based adaptation law for online parameters estimation. Thus, robustness to parametric uncertainties is achieved, which yields better accuracy as the battery ages compared to classical methods. Henceforth, accurate estimation of the battery's open circuit voltage and equivalent series resistance leads to precise state of charge and state of health determination. The stability of the closed-loop estimation scheme is guaranteed by Lyapunov's direct method unlike many online estimation methods. But, temperature is known to introduce a drift in the estimates. In this paper, a universal temperature compensation method is also proposed, a weakness of many estimation strategies in the literature. This work is one of the first attempts, if any, in achieving both SOC and SOH estimation with guaranteed stability taking into account temperature effects. The effectiveness of the proposed method is verified experimentally under different currents and temperatures.

The rest of the paper is organized as follows: Section 2 outlines the circuit model for lithium-ion batteries along with their dynamics. The proposed estimation approach along with the temperature compensation technique is detailed in Sections 3 and 4. In Section 5, experimental results are reported and discussed. We conclude with some remarks and suggestions for further studies pertaining to this problem.

2. Lithium-ion batteries

2.1. Modeling

The electric circuit model of a lithium battery is shown in Fig. 1. This model is used to describe the electrochemical phenomena such as double layer and mass transport effects. Although there is physical explanation between the electric circuit model components and the battery's chemical reactions, an equivalent circuit model is mainly established to match experimental data for a practical operating frequency range. The voltage-current characteristic dynamic mathematical model can be described by the following equations [33–35]:

$$\dot{V}_p = \frac{1}{RC} V_p - \frac{1}{C} I_b \quad (1)$$

$$V_b = V_{oc} + V_p + R_b I_b \quad (2)$$

where V_{oc} is the open circuit voltage, V_b and I_b are respectively the voltage and the current at battery terminals, R_b is the internal resistance, R and C are the equivalent resistance and capacitance, respectively, and V_p is the voltage across the RC network.

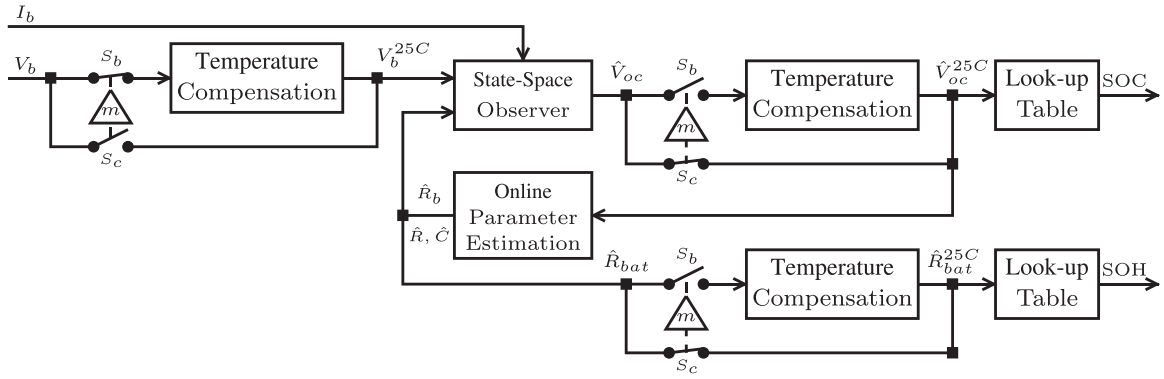


Fig. 2. Block diagram of the proposed estimation scheme.

2.2. Problem statement

The aim is to estimate the open circuit voltage and the battery's equivalent series resistance since they are directly correlated to the battery's state of charge and state of health. This is to be achieved by assuming *a priori* unknown parameters R , C , and R_b . In this work, V_p is assumed to be not measurable. The system's measurable states are the battery voltage V_b and current I_b . The current I_b is taken as positive in charge mode and negative otherwise.

Assumption 1. The battery voltage V_b and current I_b along with their derivatives \dot{V}_b and \dot{I}_b are continuous and bounded.

Assumption 2. The estimation algorithm sampling frequency is high enough such that the variation of the battery's parameters between two samples is negligible.

3. SOC estimation and online parameter identification

The proposed estimation scheme is presented in Fig. 2. As it is illustrated, the hybrid estimation strategy consists of a state-space observer and an online parameter estimator with temperature compensation. SOC Estimation is achieved with a reduced-order observer using OCV-SOC characterization. But, the knowledge of the system's parameters are required. Thus, online parameter identification is carried out using an adaptive estimator to estimate the battery's parameters including equivalent series resistance that is used for SOH estimation. Since temperature introduces a drift, a fore-compensation technique is proposed on the battery's voltage when the switch S_b is closed. Alternatively, a post-compensation is also suggested on the parameters estimate when the switch S_c is closed. It is noteworthy that the mechanical interlock between both switches allows the selection of only one temperature compensation strategy. Design details are discussed in next section. Finally, the battery's OCV and equivalent series resistance estimates \hat{V}_{oc} and \hat{R}_{bat} are used as inputs to look-up tables to estimate SOC and SOH, respectively.

3.1. Observer-based SOC estimation

Since the OCV is directly correlated with the state of charge of the battery, V_{oc} is therefore used to estimate the state of charge [34]. Henceforth, a precise OCV estimate leads to accurate SOC estimation. Substituting V_p from (2) into (1) and using assumption 2:

$$\dot{V}_b = \frac{1}{RC}V_b + R_b\dot{I}_b - \left(\frac{R_b}{RC} + \frac{1}{C} \right)I_b - \frac{1}{RC}V_{oc} \quad (3)$$

Therefore, the system's dynamics can be written in a state-space form,

$$\dot{x} = Ax + Bu \quad (4)$$

$$y = Cx \quad (5)$$

where $x \in \mathbb{R}^2 = [V_b, V_{oc}]^T$ is the state vector, $u \in \mathbb{R}^2 = [I_b, \dot{I}_b]^T$ is the input vector and $A \in \mathbb{R}^{2 \times 2}$, $B \in \mathbb{R}^{2 \times 2}$, and $C \in \mathbb{R}^2$ are given by,

$$A = \begin{bmatrix} \frac{1}{RC} & -\frac{1}{RC} \\ 0 & 0 \end{bmatrix}$$

$$B = \begin{bmatrix} -\frac{R_b + R}{RC} & R_b \\ 0 & 0 \end{bmatrix}$$

$$C = [1 \ 0]$$

Therefore, the state-space observer is defined as,

$$\dot{\hat{x}} = A\hat{x} + Bu + G(C\hat{x} - y) \quad (6)$$

$$\hat{y} = C\hat{x} \quad (7)$$

with, G being the observer gain matrix. The state-space observer estimation error is defined as,

$$e_x = \hat{x} - x \quad (8)$$

Take the derivative of e and substitute for \dot{x} and $\dot{\hat{x}}$,

$$\dot{e}_x = A\hat{x} + Bu + G(C\hat{x} - y) - Ax - Bu \quad (9)$$

Therefore, the observer dynamics is governed by,

$$\dot{e}_x = A_ce_x \quad (10)$$

where $A_c = (A + GC)$ is a Hurwitz matrix. Therefore, G can be chosen to make the eigenvalues of the matrix $(A + GC)$ all have negative real parts such that,

$$e_x(t) = e^{(A+GC)t}e_x(t_0) \rightarrow 0 \quad (11)$$

as $t \rightarrow \infty$. The observer gain matrix G can be found by solving the algebraic Riccati equation or by using a pole placement technique. It is important to note that similar to many SOC estimation techniques, the proposed state-space observer also requires the knowledge of the system's parameters, i.e., R_b , R , C . But, the battery's internal resistance and capacitance are known to vary respectively with the SOC and aging. Then, designing an observer based on presumably accurate parameters' knowledge cannot be applied efficiently in this case [14]. Unlike these strategies, the following

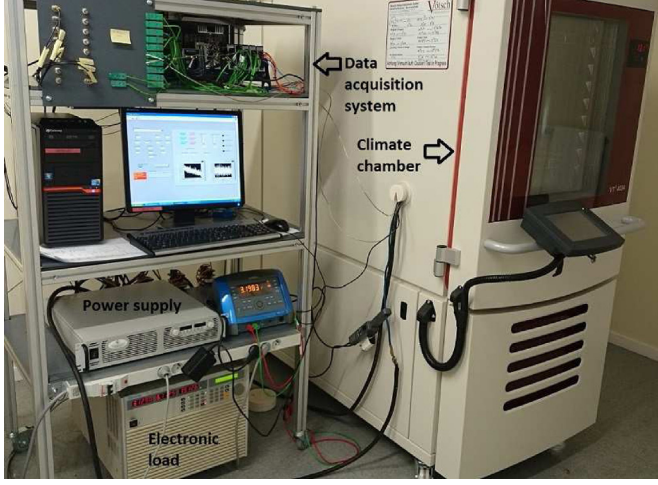


Fig. 3. Experimental setup.

section presents an online parameter estimation technique to track the parameters variation.

3.2. Online parameter identification

In here, an adaptive parameter estimator is proposed based on adaptive control theory to estimate online the battery's parameters. Henceforth, the proposed strategy's stability is guaranteed by Lyapunov's direct method. Multiplying (3) by RC yields,

$$V_b = RC\dot{V}_b - R_bRC\dot{I}_b + (R + R_b)I_b + V_{oc} = \Phi^T W \quad (12)$$

Since the OCV is assumed to be unknown, only its estimate \hat{V}_{oc} provided by the state-space observer described in the previous section can be used by the adaptive parameter estimator. Then, the model (12) can be represented by a regression model,

$$RC\dot{V}_b - R_bRC\dot{I}_b + (R + R_b)I_b + \hat{V}_{oc} = \hat{\Phi}^T W \quad (13)$$

where $\Phi \in \mathbb{R}^4$ is a vector of known functions (regressor), and $W \in \mathbb{R}^4$ is a vector of parameters:

$$W_1 = RC \quad (14)$$

$$W_2 = -R_bRC \quad (15)$$

$$W_3 = R + R_b \quad (16)$$

$$W_4 = 1 \quad (17)$$

Define the battery voltage estimation error as,

$$e_b = V_b - \hat{V}_b \quad (18)$$

Therefore, the battery voltage estimation law is expressed as follows:

$$\hat{V}_b = \hat{\Phi}^T \hat{W} - K_d e_b - e_b \quad (19)$$

where K_d is a strictly positive constant gain.

Theorem 1. Consider a nonlinear system in the form of (1) and (2) with the estimation law (19). The closed-loop system's estimation stability is achieved with the following adaptation law:

$$\dot{\hat{W}} = -\Gamma \hat{\Phi} e_b \quad (20)$$

where $\Gamma = [\gamma_1, \gamma_2, \dots, \gamma_4]$ and γ_i is a positive constant gain.

Proof 1. Choose the following Lyapunov candidate:

$$V = \frac{1}{2} \{RCe_b^2 + \tilde{W}^T \Gamma^{-1} \tilde{W}\} \quad (21)$$

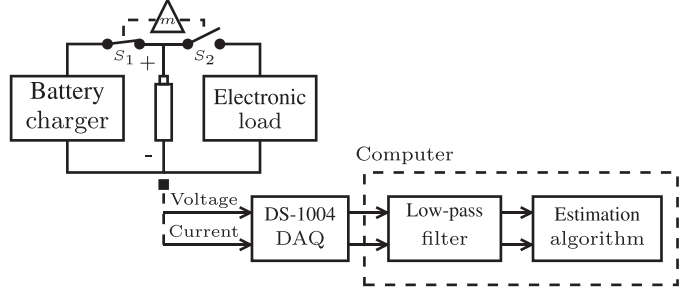
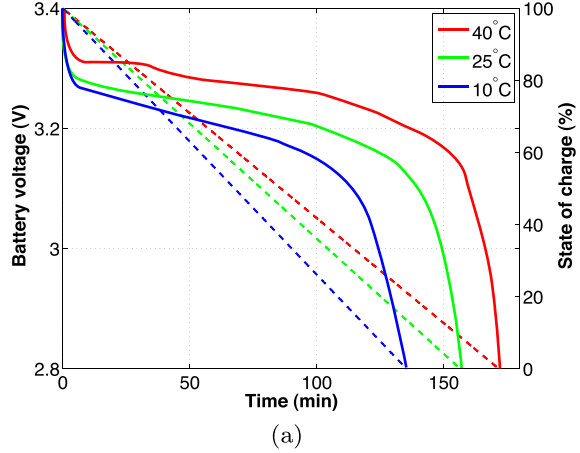
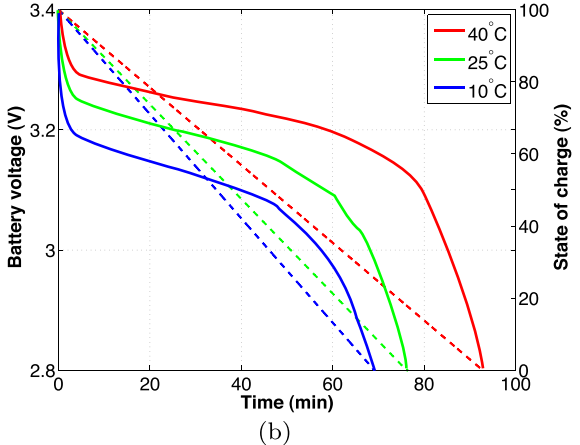


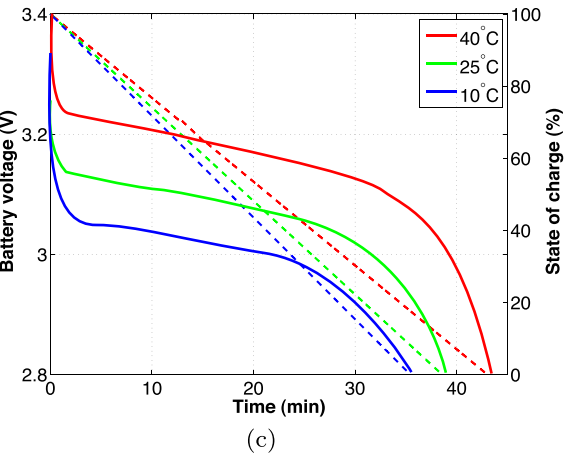
Fig. 4. Illustration of the experimental setup.



(a)



(b)



(c)

Fig. 5. Experimental results for V_b and SOC with a discharge current of: (a) 6 A; (b) 10 A; and (c) 20 A.

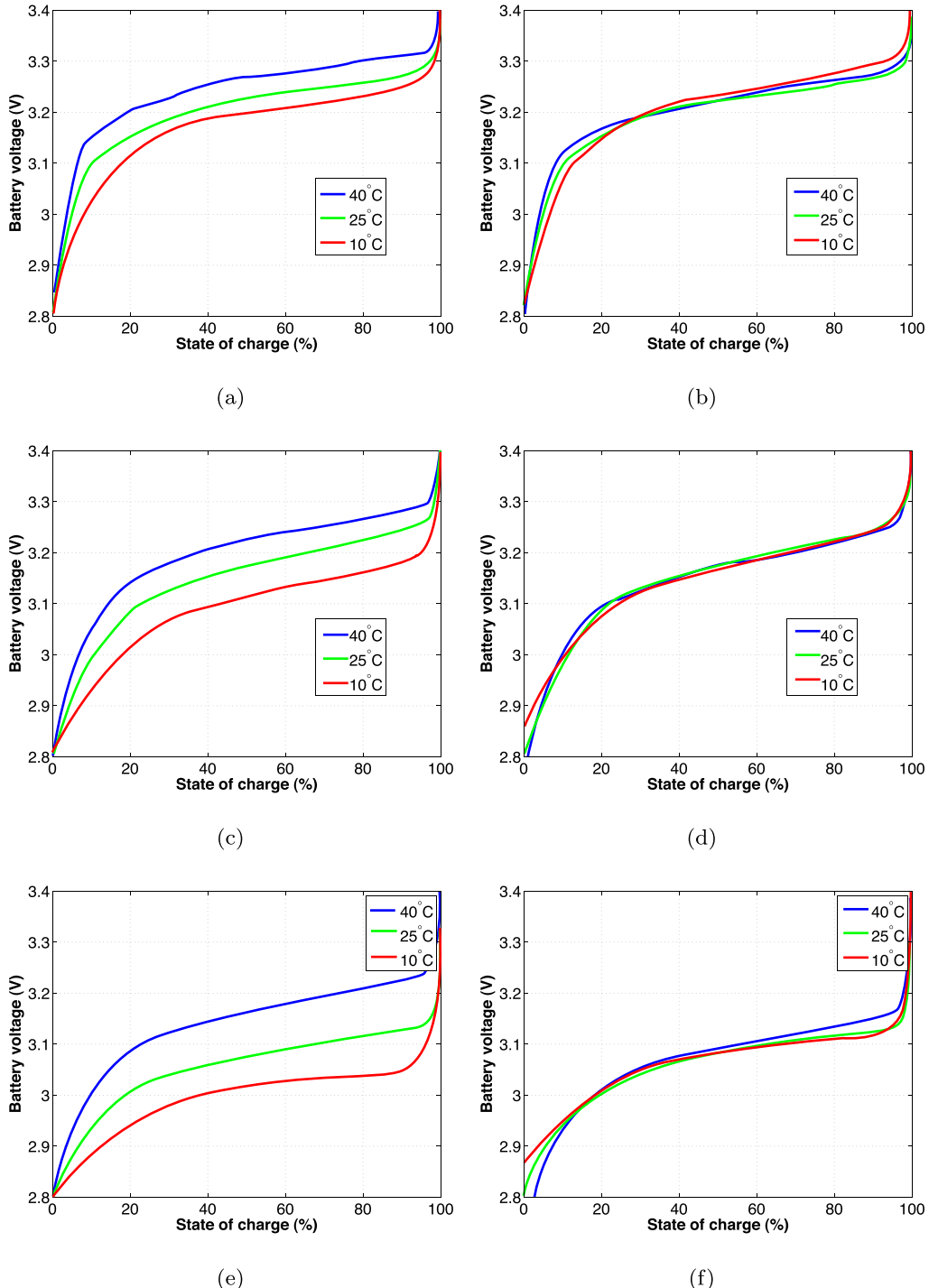


Fig. 6. Experimental results for V_b vs. SOC before and after fore-compensation with a discharge current of: (a) and (b) 6 A; (c) and (d) 10 A; and (e) and (f) 20 A.

where $\tilde{W} = \hat{W} - W$. Taking the derivative of V yields:

$$\dot{V} = R\dot{e}_b e_b + \tilde{W}^T \Gamma^{-1} \dot{\hat{W}} \quad (22)$$

Since the estimation algorithm sampling frequency is high enough such that the variation of the battery's parameter vector W between two samples is negligible (assumption 2), therefore, $\dot{\hat{W}} = \dot{W}$. Take the time derivative of (18) and Multiply both sides by RC yields:

$$R\dot{C}\dot{e}_b = R\dot{C}\dot{V}_b - R\dot{C}\dot{\hat{V}}_b \quad (23)$$

Substitute $R\dot{C}\dot{V}_b$ from (12):

$$R\dot{C}\dot{e}_b = -R\dot{C}\dot{\hat{V}}_b + R_b R\dot{C}\dot{I}_b - (R + R_b)I_b - V_{oc} + V_b \quad (24)$$

Add and subtract \hat{V}_{oc} with the use of the linear regression (13) yields:

$$R\dot{C}\dot{e}_b = V_b - \hat{\Phi}^T W + \tilde{V}_{oc} \quad (25)$$

where $\tilde{V}_{oc} = \hat{V}_{oc} - V_{oc}$ is the state-space observer error. Add and subtract e_b ,

$$R\dot{C}\dot{e}_b = \hat{V}_b - \hat{\Phi}^T W + \tilde{V}_{oc} + e_b \quad (26)$$

Set the estimation law \hat{V}_b as defined in (19):

$$RC\dot{e}_b = \hat{\Phi}^T \tilde{W} + \tilde{V}_{oc} - K_d e_b \quad (27)$$

Substitute $RC\dot{e}_b$ from (27) into (22):

$$\dot{V} = \hat{\Phi}^T \tilde{W} e_b + \tilde{W}^T \Gamma^{-1} \dot{W} + \tilde{V}_{oc} e_b - K_d e_b^2 \quad (28)$$

Setting the adaptation law as defined in (20) leads to

$$\dot{V} = \tilde{V}_{oc} e_b - K_d e_b^2 \quad (29)$$

Recall Young's inequality [36],

$$2ab \leq \frac{1}{\alpha} a^2 + \alpha b^2 \quad \forall a, b \in \mathbb{R} \text{ and } \forall \alpha > 0 \quad (30)$$

Therefore,

$$\dot{V} \leq \frac{1}{2\alpha} \tilde{V}_{oc}^2 + \frac{\alpha}{2} e_b^2 - K_d e_b^2 \quad (31)$$

Set $K_d = \frac{\alpha}{2} + \beta$ yields,

$$\dot{V} \leq \frac{1}{2\alpha} \tilde{V}_{oc}^2 - \beta e_b^2 \quad (32)$$

It is possible to choose $\alpha > 0$ and $\beta > 0$ so that $\dot{V} \leq 0$, except possibly in a neighborhood of $e_b = 0$. Then, the system is stable in the sense of Lyapunov. The neighborhood of $e_b = 0$ is a region defined by the state-space observer estimation error \tilde{V}_{oc} and gets smaller as \tilde{V}_{oc} , i.e., $e_x \rightarrow 0$. \square

4. SOH estimation and temperature compensation

4.1. SOH estimation

SOH estimation is essential to determine the battery's EOL. Generally, SOH estimation is achieved offline by capacity check using AC signal injection. But, this procedure requires the interruption of the system's operation along with additional measurement hardware and costly analysis instrumentation [37]. Another rational way that does not necessitate the use of additional hardware consists of monitoring the time needed for a fully charged battery to get discharged under a constant current. Again, this has to be performed offline and it takes several minutes or hours to fully discharge a battery and get data regarding actual capacity. Unlike these offline techniques, the proposed strategy achieves online SOH estimation with equivalent series resistance measurement while the battery is in normal operation, which eliminates constraints with respect to other procedures. Various online estimation methods are proposed in the literature. But, very few of them provide stability analysis and take into account temperature effects. These studies have reported a battery equivalent series resistance R_{bat} increase as an indication of SOH decline [38,39], which is estimated by,

$$R_{bat} = R_b + R = W_3 \quad (33)$$

Therefore, the estimation of the parameter W_3 by the online parameter estimation strategy presented in the previous section leads to estimation of the battery's equivalent series resistance R_{bat} . Then, a battery's EOL equivalent series resistance R_{EOL} is taken as 160% brand new battery's equivalent series resistance R_{new} [7,40] (i.e., $R_{EOL} = R_{new} \times 160\%$). Thus, SOH is expressed as,

$$SOH(\%) = \frac{R_{EOL} - R_{bat}}{R_{EOL} - R_{new}} \times 100\% \quad (34)$$

On another aspect, it is noteworthy that accurate SOC and SOH estimation is guaranteed since the adaptive parameter estimator tracks the battery's parameters as they vary over time.

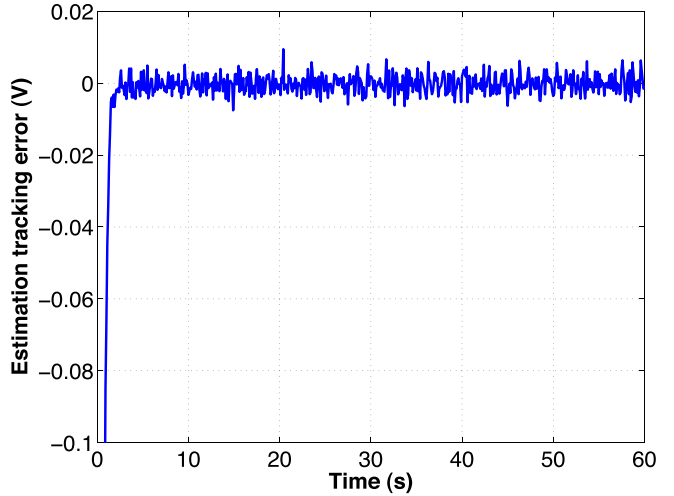


Fig. 7. Voltage estimation tracking error.

4.2. Temperature compensation

The effect of temperature variations on the battery's parameters has been extensively studied and results report a significant increase in ohmic and polarization resistances as temperature decreases [41]. As indicated by the battery's manufacturer, The SOC is defined using the OCV-SOC curve at a temperature of 25 °C. Since temperature variation introduces an offset in both V_b -SOC and OCV-SOC curves as well as in the equivalent series resistance R_{bat} , temperature compensation is then required before SOC and SOH can be determined using the battery's manufacturer look-up tables. As such, any value of SOC and SOH between 0% and 100% is defined with respect to a single reference (25 °C). Unlike other techniques, where the effect of temperature is embedded in the system's model [42,43], this paper proposes a universal compensation technique, which yields complexity reduction. Therefore, temperature compensation is carried out as,

$$\bullet^{25^\circ\text{C}} = \bullet^{actual} - \eta \Delta T \quad (35)$$

where $\Delta T = T_{actual} - 25^\circ\text{C}$, η is the compensation constant gain, \bullet^{actual} is the actual value to be corrected, and $\bullet^{25^\circ\text{C}}$ is the corrected value at 25 °C (77 °F) after the temperature compensation. It is noteworthy that the compensation strategy can be used with several estimation algorithms since the symbol \bullet can be either V_b for a fore-compensation or \hat{V}_{oc} and \hat{R}_{bat} for a post-compensation. As it is illustrated in Fig. 2, the compensation is applied to the battery's voltage V_b when S_b is closed and S_c is open and to the battery's OCV and equivalent series resistance estimates \hat{V}_{oc} and \hat{R}_{bat} when S_b is open and S_c is closed. Experimental data for V_b , \hat{V}_{oc} , and \hat{R}_{bat} are obtained at different temperatures and the corresponding compensation coefficient η is extracted to fit each experimental data.

5. Experimental results

5.1. Setup

In this work, a 20Ah, 3.2V lithium-ion phosphate battery (LiFePO₄) is used to validate the proposed approach. For that, the HIL testbench shown in Fig. 3 is designed to charge and discharge the battery. At each discharge cycle, the battery's voltage is measured at different operating temperatures using a USB-based data acquisition board (NI USB-6008) as an interface with the LiFePO₄ battery (Fig. 4). Therefore, the validation process consists of placing the battery inside a climatic chamber and characterized it at

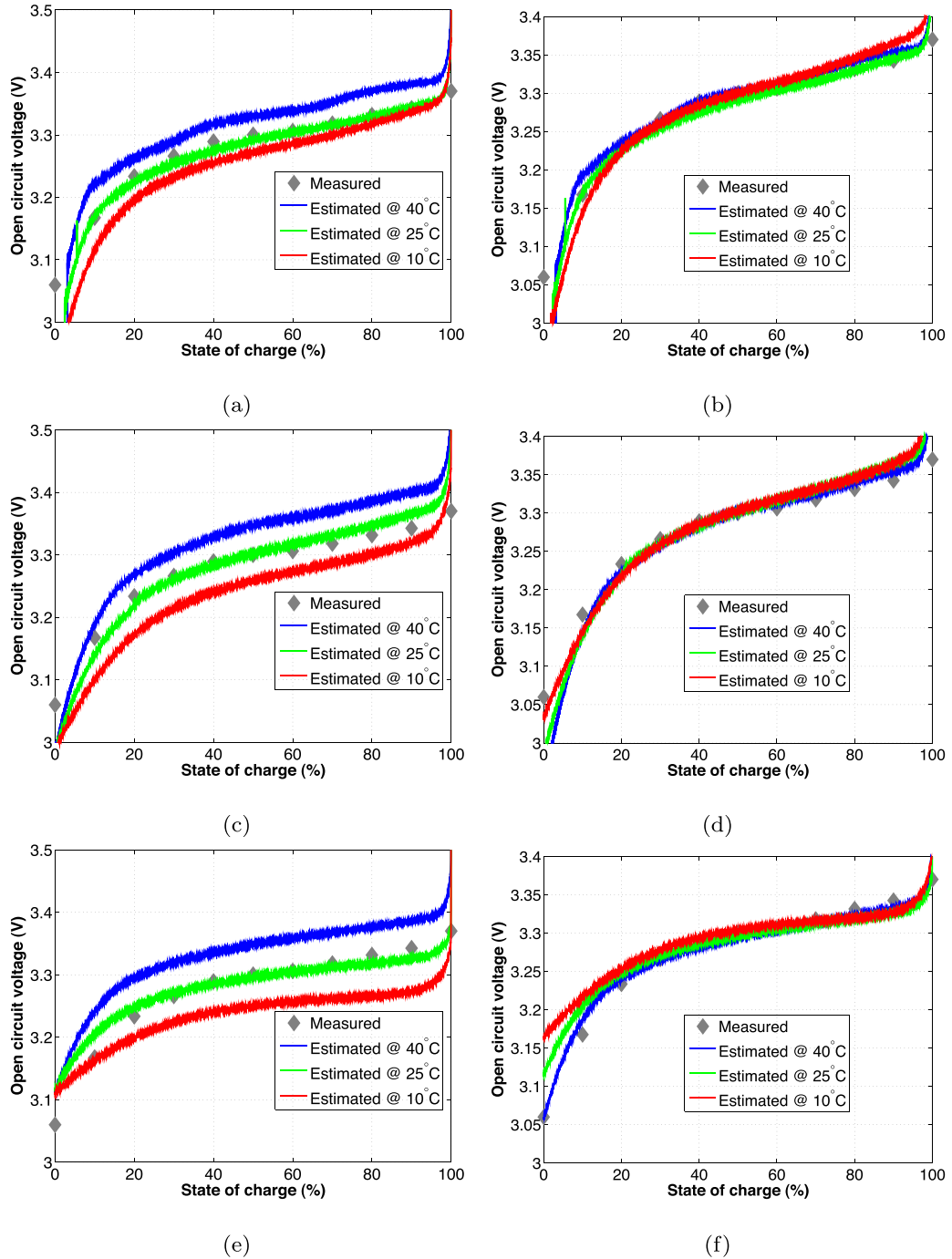


Fig. 8. Experimental results for OCV estimate with a discharge current of: (a) and (b) 6 A; (c) and (d) 10 A; and (e) and (f) 20 A.

different currents (6 A, 10 A, and 20 A) and temperatures (10 °C, 25 °C, and 40 °C). The characterization protocol consists of charging the battery according the manufacturer's guidelines, i.e., CCCV. As such, the battery is charged to 3.65 V using a constant current and then a constant voltage of 3.65 V is applied until the battery's current reaches 0.01 A, which indicated a fully charged battery. Next, the battery is fully discharge using continuous discharging until its voltage reaches 2.8 V. For every discharge current (6 A, 10 A, and 20 A), the battery's voltage is measured. These steps are repeated for different temperatures (10 °C, 25 °C, and 40 °C). In order to validate the effectiveness of the proposed approach, the necessary time to discharge the battery by a 10% is calculated. Then, the battery is discharged each time by a 10% step for each discharge current and is left at idle for about 1 h to reach equilibrium before its OCV is

measured. As for the battery's internal resistance, it is calculated as defined by [40],

$$R_{bat}(SOC) = \frac{OCV(SOC) - V_{bat}(SOC)}{I_{bat}(SOC)} \quad (36)$$

Although this method is known for its sensitivity to sensors' noise, it is sufficient to provide an approximation of the battery's resistance to validate the proposed online parameter estimation technique. Therefore, the OCV and R_{bat} measurements are compared against their estimated counterparts provided by the proposed estimation method. The algorithm sampling time is set to 0.1 sec, which yields reduced computation burden. The compensation coefficient η is set to 3.2×10^{-3} , 3×10^{-3} , and 6×10^{-5} for the battery's voltage, OCV, and resistance, respectively.

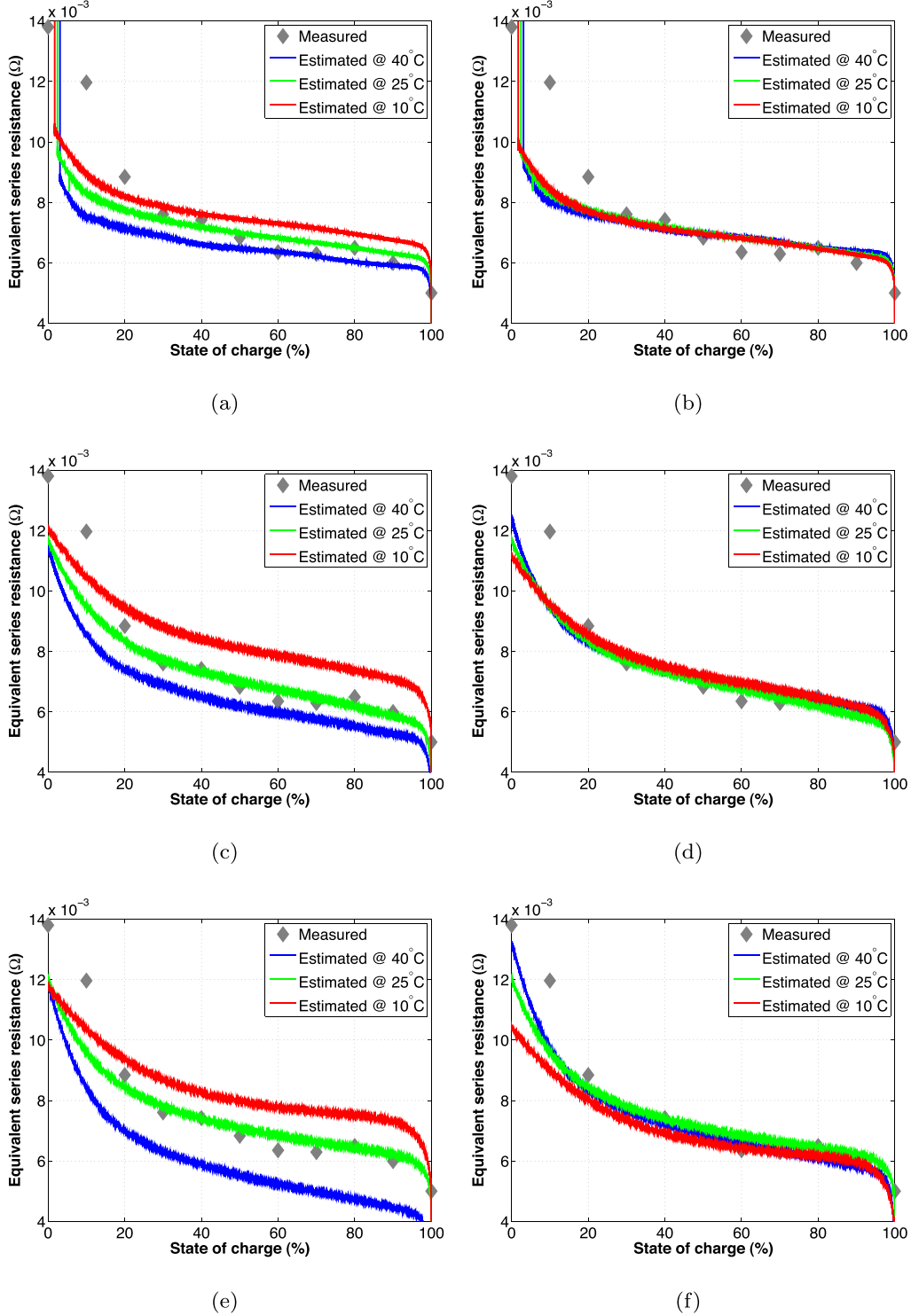


Fig. 9. Experimental results for R_{bar} estimate with a discharge current of: (a) and (b) 6 A; (c) and (d) 10 A; and (e) and (f) 20 A.

5.2. Results

To study the temperature's effect, the battery's voltage and SOC for a discharge current of 6 A, 10 A, and 20 A at different temperatures are depicted in Fig. 5(a)–(c). It is important to note that temperature introduces an offset on the battery's voltage. The battery's voltage vs. the SOC, called V_{bat} -SOC curve, is established as shown in Fig. 6(a), (c), and (e) for various temperatures to validate the proposed estimation scheme. The performance of the proposed

temperature compensation method when applied to the battery's voltage V_b (i.e., S_b is closed and S_c is open) is depicted in Fig. 6(b), (d), and (f). As it can be observed, the proposed technique is able to compensate for the drift introduced by temperature variations.

Next, three sets of experiments are carried-out to study the performance of the proposed estimation scheme. The system's response is studied taking into account the OCV estimate $W_4 \approx V_{\text{oc}}$, and the battery's equivalent series resistance $W_3 \approx R_{\text{bat}}$. Since the tracking error behavior is similar for all temperatures, it is then

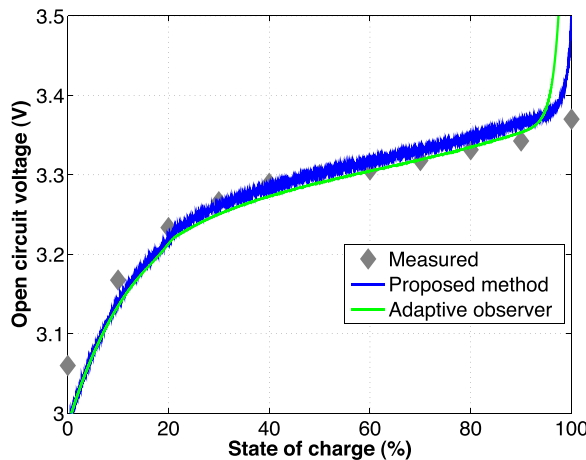


Fig. 10. Comparison against the adaptive observer in [16].

shown in Fig. 7 only for one case (10 A at 25 °C) and for the first 60 s to highlight convergence at start-up. The battery's parameter estimation vector is initialized to zero, which yields significant start-up error to better show the convergence properties of the estimation algorithm. As it is illustrated, the battery's estimation tracking error decreases gradually to a negligible magnitude. The advantage behind the use of the proposed estimation scheme is clearly shown in this experiment. As it is illustrated in the results depicted in Fig. 8, the OCV estimate decreases as the battery gradually discharges. The OCV-SOC curve is then established. Since temperature introduced a drift on the OCV estimate, the temperature compensation is applied (i.e., S_b is open and S_c is closed). As it is illustrated in Fig. 8(b), (d), and (f), good temperature compensation performance is achieved. Comparison with measured OCV values highlight the high accuracy of the proposed approach. Experimental results for R_{bat} estimation are depicted in Fig. 9. As it is expected, the battery's equivalent series resistance increases as the battery discharges. Again, a drift is observed due to temperature variations. Then, the proposed temperature compensation technique is applied to overcome this effect as it is shown for in Fig. 9(a), (c), and (e). Therefore, a mapping to the SOC and SOH can be performed using look-up tables. It is noteworthy that low battery's resistance values combined with low sensors' precision and measurements' noise make accurate estimation a difficult task to undertake and many estimation procedures fail to predict SOH with high accuracy [44]. Nevertheless, good performance is achieved in the linear SOC portion.

Then, the adaptive observer proposed in [16] is implemented and used as a benchmark for comparison. Results for a discharge current of 10 A at 25 °C are presented in Fig. 10. Performance for the other discharge currents and temperatures is similar and thus, their results are omitted for brevity. As it is revealed by the comparison results, both methods show negligible difference as they yield accurate OCV estimation compared to the measured OCV.

6. Conclusion

In this paper, a hybrid estimator is introduced for lithium-ion batteries. The proposed strategy combines between the capabilities of adaptive control theory and state-space observer to achieve high estimation accuracy in the presence of parametric uncertainties. The estimator's performance shows that the battery's OCV can be determined with high accuracy. Furthermore, the convergence and stability of the proposed closed-loop estimation scheme is guaranteed by Lyapunov's direct method. Moreover, its implementation is easier as opposed to other advanced estimation approaches, such as intelligent estimators. The proposed online estimation approach

can be applied to lithium-ion batteries subjected to temperature uncertainties and is more suitable for real-time applications, such as electric/hybrid vehicles. Experimental results highlight the performance of the proposed estimation scheme in tracking the battery's parameters that are usually used as SOC and SOH indicators. Additionally, the proposed universal compensation strategy demonstrates its effectiveness in dealing with temperature variation effects. Furthermore, comparison against an adaptive observer is presented as a benchmark to better highlight the estimation accuracy.

References

- [1] M.-Y. Kim, C.-H. Kim, J.-H. Kim, G.-W. Moon, A chain structure of switched capacitor for improved cell balancing speed of lithium-ion batteries, *IEEE Trans. Ind. Electron.* 61 (8) (2014) 3989–3999.
- [2] A. Kuperman, U. Levy, J. Goren, A. Zafransky, A. Savernin, Battery charger for electric vehicle traction battery switch station, *IEEE Trans. Ind. Electron.* 60 (12) (2013) 5391–5399.
- [3] A. Ranjbar, A. Banaei, A. Khoobroo, B. Fahimi, Online estimation of state of charge in Li-ion batteries using impulse response concept, *IEEE Trans. Smart Grid* 3 (1) (2012) 360–367.
- [4] T. Hansen, C.-J. Wang, Support vector based battery state of charge estimator, *J. Power Sources* 141 (2) (2005) 351–358.
- [5] S. Duryea, S. Islam, W. Lawrence, A battery management system for stand-alone photovoltaic energy systems, *IEEE Ind. Appl. Mag.* 7 (3) (2001) 67–72.
- [6] L. Liu, L. Wang, Z. Chen, C. Wang, F. Lin, H. Wang, Integrated system identification and state-of-charge estimation of battery systems, *IEEE Trans. Energy Convers.* 28 (1) (2013) 12–23.
- [7] M. Gholizadeh, F. Salmasi, Estimation of state of charge, unknown nonlinearities, and state of health of a lithium-ion battery based on a comprehensive unobservable model, *IEEE Trans. Ind. Electron.* 61 (3) (2014) 1335–1344.
- [8] M. Shahriari, M. Farrokhi, Online state-of-health estimation of VRLA batteries using state of charge, *IEEE Trans. Ind. Electron.* 60 (1) (2013) 191–202.
- [9] Z. Chen, Y. Fu, C. Mi, State of charge estimation of lithium-ion batteries in electric drive vehicles using extended Kalman filtering, *IEEE Trans. Veh. Technol.* 62 (3) (2013) 1020–1030.
- [10] H. He, R. Xiong, X. Zhang, F.S. and, J. Fan, State-of-charge estimation of the lithium-ion battery using an adaptive extended Kalman filter based on an improved Thevenin model, *IEEE Trans. Veh. Technol.* 60 (4) (2011) 1461–1469.
- [11] I.-S. Kim, Nonlinear state of charge estimator for hybrid electric vehicle battery, *IEEE Trans. Power Electron.* 23 (4) (2008) 2027–2034.
- [12] A. Szumanowski, Y. Chang, Battery management system based on battery nonlinear dynamics modeling, *IEEE Trans. Veh. Technol.* 57 (3) (2008) 1425–1432.
- [13] P. van Bree, A. Veltman, W. Hendrix, P. van den Bosch, Prediction of battery behavior subject to high-rate partial state of charge, *IEEE Trans. Veh. Technol.* 58 (2) (2009) 588–595.
- [14] H. Chaoui, P. Sicard, Accurate state of charge (SOC) estimation for batteries using a reduced-order observer, in: *IEEE International Conference on Industrial Technology & Southeastern Symposium on System Theory*, 2011, pp. 39–43.
- [15] H. Chaoui, P. Sicard, H. Ndjana, Adaptive state of charge (SOC) estimation for batteries with parametric uncertainties, in: *IEEE/ASME Advanced Intelligent Mechatronics International Conference*, 2010, pp. 703–707.
- [16] H. Chaoui, N. Golbon, I. Hmouz, R. Souissi, S. Tahar, Lyapunov-based adaptive state of charge and state of health estimation for lithium-ion batteries, *IEEE Trans. Ind. Electron.* 62 (3) (2015) 1610–1618.
- [17] J. Xu, C. Mi, B. Cao, J. Deng, Z. Chen, S. Li, The state of charge estimation of lithium-ion batteries based on a proportional-integral observer, *IEEE Trans. Veh. Technol.* 63 (4) (2014) 1614–1621.
- [18] N. Watrin, R. Roche, H. Ostermann, B. Blunier, A. Miraoui, Multiphysical lithium-based battery model for use in state-of-charge determination, *IEEE Trans. Veh. Technol.* 61 (8) (2012) 3420–3429.
- [19] A.E. Mejdoubi, A. Oukaour, H. Chaoui, Y. Slamani, J. Sabor, H. Gualous, Online supercapacitor diagnosis for electric vehicle applications, *IEEE Trans. Veh. Technol.* 65 (6) (2016) 4241–4252.
- [20] R. Xiong, H. He, F. Sun, K. Zhao, Evaluation on state of charge estimation of batteries with adaptive extended Kalman filter by experiment approach, *IEEE Trans. Veh. Technol.* 62 (1) (2013) 108–117.
- [21] C. Weng, J. Sun, H. Peng, Model parameterization and adaptation based on the invariance of support vectors with applications to battery state-of-health monitoring, *IEEE Trans. Veh. Technol.* 64 (9) (2015) 3908–3917.
- [22] D. Howey, P. Mitcheson, V. Yufit, G. Offer, N. Brandon, Online measurement of battery impedance using motor controller excitation, *IEEE Trans. Veh. Technol.* 63 (6) (2014) 2557–2566.
- [23] G. M, L. Y, H. Z, Battery state of charge online estimation based on particle filter, in: *Fourth International Congress on Image and Signal Processing*, Shanghai, China 2011, 2233–2236.

- [24] J. Li, J. Klee Barillas, C. Guenther, M. Danzer, Sequential Monte Carlo filter for state estimation of LiFePO₄ batteries based on an online updated model, *J. Power Sources* 247 (2014) 156–162.
- [25] S. Schwunk, N. Armbruster, S. Straub, J. Kehl, M. Vetter, Particle filter for state of charge and state of health estimation for lithium-iron phosphate batteries, *J. Power Sources* 239 (2013) 705–710.
- [26] H. Chaoui, P. Sicard, Adaptive fuzzy logic control of permanent magnet synchronous machines with nonlinear friction, *IEEE Trans. Ind. Electron.* 59 (2) (2012) 1123–1133.
- [27] H. Chaoui, W. Gueaieb, Type-2 fuzzy logic control of a flexible-joint manipulator, *J. Intell. Robot. Syst.* 51 (2) (2008) 159–186.
- [28] H. Chaoui, P. Sicard, W. Gueaieb, ANN-based adaptive control of robotic manipulators with friction and joint elasticity, *IEEE Trans. Ind. Electron.* 56 (8) (2009) 3174–3187.
- [29] H. Chaoui, P. Sicard, Robust ANN-based nonlinear speed observer for permanent magnet synchronous machine drives, in: *IEEE International Conference on Electric Machines and Drives*, 2011, pp. 587–592.
- [30] M. Charkhgard, M. Farrokhi, State-of-charge estimation for lithium-ion batteries using neural networks and EKF, *IEEE Trans. Ind. Electron.* 57 (12) (2010) 4178–4187.
- [31] H.-T. Lin, T.-J. Liang, S.-M. Chen, Estimation of battery state of health using probabilistic neural network, *IEEE Trans. Ind. Inf.* 9 (2) (2013) 679–685.
- [32] F.-J. Lin, M.-S. Huang, P.-Y. Yeh, H.-C. Tsai, C.-H. Kuan, DSP-based probabilistic fuzzy neural network control for Li-ion battery charger, *IEEE Trans. Power Electron.* 27 (8) (2012) 3782–3794.
- [33] J. Kim, J. Shin, C. Chun, B. Cho, Stable configuration of a Li-ion series battery pack based on a screening process for improved voltage/SOC balancing, *IEEE Trans. Power Electron.* 27 (1) (2012) 411–424.
- [34] M. Petzl, M. Danzer, Advancements in OCV measurement and analysis for lithium-ion batteries, *IEEE Trans. Energy Convers.* 28 (3) (2013) 1–7.
- [35] M. Chen, G.A. Rincon-Mora, Accurate electrical battery model capable of predicting runtime and I–V performance, *IEEE Trans. Energy Convers.* 21 (2) (2006) 504–511.
- [36] R.A. Freeman, P.V. Kokotovic, Lyapunov design, *Control Handb.* 77 (1996) 932–940.
- [37] W. Huang, J.A. Qahouq, An online battery impedance measurement method using DC–DC power converter control, *IEEE Trans. Ind. Electron.* (2014) 99.
- [38] V. Pop, H.J. Bergveld, P.P.L. Regtien, J.H.G.O. het Veld, D. Danilov, P.H.L. Notten, Battery aging and its influence in the electromotive force, *J. Electrochem. Soc.* 154 (8) (2007) A744–A750.
- [39] S. Grolleau, A. Delailler, H. Gualous, P. Gyan, R. Revel, J. Bernard, E. Redondo-Iglesias, J. Peter, Calendar aging of commercial graphite/LiFePO₄ cell – predicting capacity fade under time dependent storage conditions, *J. Power Sources* 255 (2014) 450–458.
- [40] D. Haifeng, W. Xuezhe, S. Zechang, A new SOH prediction concept for the power lithium-ion battery used on HEVs, in: *IEEE Vehicle Power and Propulsion Conference*, Dearborn, Michigan, USA, 2009, pp. 7–10.
- [41] F. Feng, R. Lu, G. Wei, C. Zhu, Identification and analysis of model parameters used for LiFePO₄ cells series battery pack at various ambient temperature, *IET Electr. Syst. Transp.* 6 (2) (2016) 50–55.
- [42] H. Rahimi-Eichi, F. Baronti, M.-Y. Chow, Online adaptive parameter identification and state-of-charge coestimation for lithium-polymer battery cells, *IEEE Trans. Ind. Electron.* 61 (4) (2014) 2053–2061.
- [43] A.E. Mejdoubi, A. Ouakour, H. Chaoui, Y. Slamani, J. Sabor, H. Gualous, State-of-charge and state-of-health lithium-ion batteries diagnosis according to surface temperature variation, *IEEE Trans. Ind. Electron.* 63 (4) (2016) 2391–2402.
- [44] H. Chaoui, A.E. Mejdoubi, A. Ouakour, H. Gualous, Online system identification for lifetime diagnostic of supercapacitors with guaranteed stability, *IEEE Trans. Control Syst. Technol.* 24 (6) (2016) 2094–2102.